LANGMUIR

pubs.acs.org/Langmuir Article

Membrane-Mimicking Reverse Micelles for High-Resolution Interfacial Study of Proteins and Membranes

Courtney L. Labrecque, Aubree L. Nolan, Angela M. Develin, Abdul J. Castillo, Adam R. Offenbacher, and Brian Fuglestad*

Cite This: *Langmuir* 2022, 38, 3676–3686 Read Online

ACCESS | Metrics & More | Article Recommendations | Supporting Information

ABSTRACT: Despite substantial advances, the study of proteins interacting with membranes remains a significant challenge. While integral membrane proteins have been a major focus of recent efforts, peripheral membrane proteins (PMPs) and their interactions with membranes and lipids have far less high-resolution information available. Their small size and the dynamic nature of their interactions have stalled detailed interfacial study using structural methods like cryo-EM and X-ray crystallography. A major roadblock for the structural analysis of PMP interactions is limitations in membrane models to study the membrane recruited state. Commonly used membrane mimics such as liposomes, bicelles, nanodiscs, and micelles are either very large or composed of non-biological detergents, limiting their utility for the NMR study of PMPs. While there have been previous successes with integral and peripheral membrane proteins, currently employed reverse micelle (RM) compositions are optimized for their inertness with proteins rather than their ability to mimic membranes. Applying more native, membrane-like lipids and surfactants promises to be a valuable advancement for the study of interfacial interactions between proteins and membranes. Here, we describe the development of phosphocholine-based RM systems that mimic biological membranes and are compatible with high-resolution protein NMR. We demonstrate new formulations that are able to encapsulate the model soluble protein, ubiquitin, with minimal perturbations of the protein structure. Furthermore, one formula, DLPC:DPC, allowed the encapsulation of the PMPs glutathione peroxidase 4 (GPx4) and phosphatidylethanolamine-binding protein 1 (PEBP1) and enabled the embedment of these proteins, matching the expected interactions with biological membranes. Dynamic light scattering and small-angle X-ray scattering characterization of the RMs reveals small, approximately spherical, and non-aggregated particles, a prerequisite for protein NMR and other avenues of study. The formulations presented here represent a new tool for the study of elusive PMP interactions and other membrane interfacial investigations.

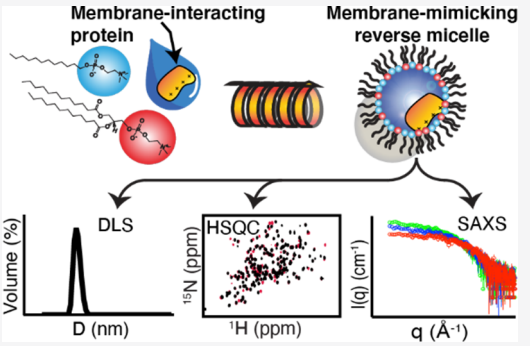

INTRODUCTION

Membranes and their associated proteins serve as the gatekeepers to cells. Though fundamental to cellular function, interactions at the membrane interface have lagged in high-resolution experimentation, leaving broad blind spots in our understanding.[1] While the advancement of cryo-EM has proven to be a revolution in understanding membrane protein structures, these views are generally static and do not reflect dynamic or equilibria processes.[2] Additionally, a highly diverse and important class of membrane proteins, peripheral membrane proteins (PMPs), are often too small to study using cryo-EM methods.[3] PMPs are generally water-soluble, globular proteins that attach to cellular membrane surfaces to perform their function.[4,5] The soluble state of PMPs is often easily studied using X-ray crystallography, but the characterization of membrane embedment and engagement with lipid substrates is generally inaccessible.[6] Detergent-based micelles, bicelles, and nanodiscs are established membrane models that have allowed high-resolution study of protein interactions with membranes using NMR.[7] Despite the benefits of studying protein−membrane interactions using these tools, some major drawbacks remain. Some detergent assemblies, namely, bicelles and nanodiscs, are relatively large, making their use in protein NMR cumbersome and somewhat limited.[8] Micelles, while smaller, are constructed from highly artificial detergents, which can have a profound effect on the protein structure and stability, limiting their compatibility with many protein systems.[9,10] Reverse micelles (RMs) have been utilized to mimic biological membranes in a variety of studies and are compatible with high-resolution protein study using NMR.[11] RMs are composed of a small, nanoscale pool of water encased

Received: November 17, 2021
Revised: January 25, 2022
Published: March 17, 2022

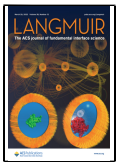

https://doi.org/10.1021/acs.langmuir.1c03085
Langmuir 2022, 38, 3676−3686

in a shell of surfactants, with the polar headgroups forming an interface with water and the apolar tails pointing outward toward a hydrophobic solvent. The amphipathic composition of RMs can allow interfacial studies of membrane-interacting proteins. Using a low-viscosity solvent allows for high-resolution NMR studies of proteins that are large by NMR standards.[11,12] While potentially promising, current RM formulations have been developed with primarily water-solubilized proteins in mind. Further enhancement is needed to fully utilize RMs as membrane mimics.

RMs have proven to be incredibly useful as membrane mimics for interfacial studies. Observations of the behavior of water and small molecules using a variety of methods have revealed physical and chemical properties of interfacial regions.[13−17] The water core of RMs serves as a host for soluble proteins, enabling functional, structural, and enzymatic investigations.[18−21] In combination with NMR methods, RM encapsulation has greatly enhanced many avenues of study. Originally developed to extend the protein NMR size limit, low-viscosity, nonpolar solvents used for protein RM encapsulation effectively prevent the spectral quality loss typically seen with very large proteins.[12] Encapsulation of proteins within the small, nanoscale RM water pool can stabilize proteins and force unfolded proteins into folded, compact conformations.[22,23] Extreme ionic strengths and high small molecule concentrations are detrimental to the spectral quality in protein NMR, but the small relative volume of the water phase within RMs eliminates this effect.[24−26] RM encapsulation has solved long-standing problems in protein studies such as measuring the atomic resolution of protein hydration dynamics and extending the detection limit in inhibitor fragment screening.[27,28] The utility of an RM formulation for use in encapsulation is determined by its ability to retain the native state of the protein. Surfactants used for protein encapsulation need to be carefully considered and tested for their ability to retain the structural fidelity of the protein.[11,29] Currently, several protein-compatible RM formulations exist and are able to encapsulate a large range of proteins for study. However, current RM formulations that have been developed for high-resolution protein study diverge significantly from the chemical composition of cellular membranes. The two common currently employed RM formulations for protein encapsulation, cetyltrimethylammonium bromide (CTAB) and the binary mixture of 1-decanoyl-*rac*-glycerol with lauryldimethylamine-*N*-oxide (10MAG:LDAO), do not mimic lipids found in cellular membranes. The amphipathic nature of the surfactant shell of these RM systems has been leveraged to embed some membrane integral or membrane-associated proteins for NMR study.[29−32] However, the trimethylamine CTAB headgroup, the glycerol 10MAG headgroup, and the dimethylamine oxide LDAO headgroup do not resemble headgroups found in natural lipids within biological membranes.[33] Though commonly used, dioctyl sulfosuccinate sodium salt (AOT) has proven to be denaturing to most proteins, limiting its use in protein encapsulation and interfacial studies.[11] This highlights the necessity of using a method that reports on the fold of the protein, such as NMR, to develop and optimize novel protein-compatible RM systems. Using surfactants that mimic the lipids found in natural membranes promises to expand the utility of RMs for protein interfacial investigations.

Here, we describe the development of RM surfactant formulations that are based on the phosphocholine-rich chemistry of human cellular membranes.[34] Inspired by previous works that utilized cellular extracted phospholipids (often referred to as lecithin), and other phosphocholine lipids and surfactants to construct RMs,[35−39] we sought to discover and validate novel, protein-compatible RM formulations using surfactants with phosphocholine headgroups. Screening revealed several surfactant mixtures that produced clear "empty" RM solutions. Using a model water-soluble protein, ubiquitin, we found three formulas capable of protein encapsulation. Since our ultimate goal was to create a membrane-mimicking RM system to study membrane interfacial interactions, we utilized two PMPs to test the ability of our formulations to mimic a phosphocholine membrane surface: human glutathione peroxidase 4 (GPx4) and human phosphatidylethanolamine-binding protein 1 (PEBP1). Among other functions, GPx4 is the only enzyme that reduces lipid hydroperoxides, a vital role in protecting cellular membranes from oxidative damage.[40] The membrane-binding interface of GPx4 has been recently measured experimentally using micelles and isotropic bicelles.[41] PEBP1, also known as Raf-1 kinase inhibitory protein, plays an important role in several physiological processes, including neuronal development, spermatogenesis, and cardiac output.[42] PEBP1 is known to engage with membranes, with bulk measurements and proposed models of the membrane interaction previously reported.[43−46] However, to our knowledge, there are no direct, high-resolution measurements of PEBP1 interactions with membranes. In the current study, we identify an RM mixture that demonstrates compatibility with GPx4 and PEBP1, a combination of 1,2-dilinoleoyl-*sn*-glycero-3-phosphocholine (DLPC) and *n*-dodecylphosphocholine (DPC), with hexanol acting as a co-surfactant. Using the DLPC:DPC binary mixture, the experimentally mapped membrane interface of GPx4 matches the binding mode previously characterized using other membrane models, confirming its usefulness as a membrane mimic. Additionally, the footprint of the interaction between the RM surface and PEBP1 was mapped, which represents the first measurement of this particular interaction that closely matches the predicted interface. Dynamic light scattering (DLS) and small-angle X-ray scattering (SAXS) revealed small, homogeneous, and approximately spherical DLPC:DPC RMs, which become larger with the increase in water content, which are key properties for optimized RM systems. DLPC:DPC RMs prove to be a robust system for protein encapsulation and are unique in their resemblance to biological membranes in comparison to other protein-compatible RM surfactants. The optimal formulation presented here proves to form RMs, is suitable for soluble protein study with high structural fidelity, provides long-term sample stability, and represents a novel tool for membrane interfacial and protein−membrane interaction studies.

EXPERIMENTAL SECTION

Surfactant Screening for RM Formation. All surfactant mixtures were initially constructed as putative "empty", or without protein, RMs using 75 or 150 mM total surfactant (Table S1). The following surfactants and mixtures were screened: DLPC, 1,-2-dioleoyl-*sn*-glycero-3-phosphocholine (DOPC), *n*-hexadecylphosphocholine (HPC), DLPC:HPC, 1,2-dihexanoyl-*sn*-glycero-3-phosphocholine (DHPC):HPC, DHPC:DPC, DLPC:1-palmitoyl-2-hydroxy-*sn*-glycero-3-phosphocholine (Lyso-PC), and DLPC:DPC. All surfactants were purchased from Avanti Polar Lipids (Birmingham, AL). All surfactant mixtures were tested with *n*-hexane (Thermo

https://doi.org/10.1021/acs.langmuir.1c03085
Langmuir 2022, 38, 3676−3686

Fisher Scientific, Waltham, MA) as the solvent and water loading (W_0) values of 10, 15, 20, and 25, defined as

$$W_0 = \frac{[\text{water}]}{[\text{surfactant}]}$$

The buffer used for empty RM screening was GPx4 NMR buffer (20 mM bis−Tris pH 6.0, 100 mM NaCl, and 20 mM DTT). Bromophenol blue was added to the buffer for ease of visualization of solution clarity. Surfactants were vacuum-dried overnight to eliminate residual water. The appropriate mass of surfactants was weighed into glass vials with *n*-hexane, and 200 mM hexanol (Sigma-Aldrich, St. Louis, MO) was added prior to the buffer to facilitate proper mixing (Figure S1a). Generally, hexanol was titrated in steps of 100 mM, samples were vortexed and sonicated in a water bath, and the clarity was assessed to construct hexanol phase diagrams.

Dynamic Light Scattering. Surfactant systems that displayed transparency from the initial screens were measured using DLS to confirm the formation of RMs and to assess dispersity. All mixtures were tested with 75 mM total surfactant, a W_0 of 20 (20 mM bis−Tris pH 6.0, 100 mM NaCl, and 20 mM DTT), and a hexanol concentration of either 1.2 M (DLPC:DPC, DOPC, DLPC, and DLPC:HPC) or 1.8 M (DHPC:DPC, DHPC:HPC, HPC, and DLPC:Lyso-PC). Experiments were performed using a Malvern Zetasizer Nano-S instrument. Published viscosity and dielectric constant parameters were used for hexane as a binary mixture of either 1.2 or 1.8 M hexanol.[47,48] For the 1.2 M hexanol:hexane mixture, the viscosity used was 0.364 mPa·s and the dielectric constant used was 2.14, while for 1.8 M hexanol:hexane, the viscosity used was 0.408 mPa·s and the dielectric constant used was 2.34. The refractive index was set to 1.38 for both conditions. The RM samples were loaded into a quartz cuvette and kept at a constant temperature of 25 °C. Each sample was scanned 12−15 times to create one measurement, and each measurement was repeated in triplicate to generate an average and error of the size measurement. In addition to the surfactant trials, increased NaCl concentration and encapsulated ubiquitin and GPx4 were tested in our ultimate formula, 75 mM DLPC:DPC, at a molar percentage ratio of 50:50. NaCl (500 mM) was used to confirm the validity of our SAXS experiments, and the protein encapsulated trials were used to confirm that the size of the RM remained generally unchanged when protein was introduced. For these additional trials, the W_0 remained the same at 20 and the hexanol concentration was 1.2 M.

Protein Production. Proteins were isotopically labeled using $^{15}NH_4Cl$ for NMR investigations, and ^{13}C-glucose was used for labeling for PEBP1 assignment experiments. Isotopes were purchased from Sigma-Aldrich (St. Louis, MO). All proteins were grown in *E. coli*, induced with isopropyl-*β*-D-1-thiogalactopyranoside (IPTG), lysed, and purified using either Ni-NTA affinity chromatography (GPx4, His-tagged ubiquitin, and PEBP1) or cation exchange chromatography (untagged ubiquitin). N-terminal poly-histidine-tags of GPx4 and PEBP1 were cleaved for the final NMR analysis. Final protein concentrations were quantified using a Bradford assay. Detailed protein preparation protocols are provided in the Supporting Information.

Protein Encapsulation in RMs. Surfactant mixtures that produced clear solutions during the initial screen and formed RMs from the DLS measurements (DLPC, DOPC, DLPC:HPC, DHPC:HPC, DHPC:DPC, HPC, DLPC:Lyso-PC, and DLPC:DPC) were used to encapsulate ubiquitin. RM formulations containing encapsulated ubiquitin were assessed by NMR spectral quality and minimal spectral shift compared to ubiquitin in aqueous conditions. Initial RM conditions were optimized by adjusting W_0 and hexanol concentration as well as the molar ratio of surfactants for the binary mixtures. The most promising ubiquitin-compatible RM formulations (DLPC, DLPC:DPC, and DLPC:HPC) were tested for ability to encapsulate GPx4. For RM formulations that encapsulated GPx4 successfully (DLPC:DPC and DLPC:HPC), further optimizations were performed such as W_0, hexanol concentration, and surfactant ratios to determine conditions that result in the highest quality protein NMR spectrum. Initial encapsulations were performed using 150 mM total surfactant, but the surfactant was later adjusted to 75 mM due to higher spectral quality. To create the RMs for NMR spectroscopy, labeled protein was concentrated to the desired volume necessary for the target W_0. For ubiquitin and GPx4, the optimal W_0 values were 15 and 20, respectively. Surfactants were vacuum-dried overnight and stored in air-tight desiccator vessels to eliminate residual water. The appropriate mass of the surfactant mixture was weighed into a glass vial to achieve 75 mM total surfactant concentration. The surfactants were initially solubilized in 500 μL of pentane (Sigma-Aldrich, St. Louis, MO) and 200 mM hexanol. Next, the protein solution was incorporated and alternatively vortexed and mixed in a sonicating water bath. Hexanol was then added 200 mM at a time, and the solutions were vortexed and sonicated until clarity was achieved, typically with >800 mM hexanol. DLPC:DPC produced the highest quality ^{15}N-HSQC spectra of encapsulated GPx4, which led us to pursue it further as our lead membrane-mimicking surfactant system. PEBP1 was encapsulated into DLPC:DPC with an optimal W_0 of 25. For GPx4 encapsulation in CTAB (Sigma-Aldrich, St. Louis, MO) and 10MAG:LDAO (Avanti Polar Lipids, Birmingham, AL) RM systems, 150 mM of the total surfactant was used for both conditions with a molar percentage ratio for 10MAG:LDAO of 60:40. The W_0 was 20 for both conditions, and hexanol titrations were performed until sample clarity was achieved (600 mM for the CTAB sample, 25 mM for the 10MAG:LDAO sample).

Micelle Sample Preparation. DPC micelle samples were assessed to compare the interfaces of GPx4 and PEBP1 as well as for stability assessments. Mass corresponding to 25 mM DPC for GPx4 and 50 mM for PEBP1 was weighed out and added to an NMR sample of either ^{15}N-GPx4 or ^{15}N-PEBP1 and 10% v/v of D_2O. The sample was vortexed until the solution was clear, and NMR spectra were collected. Spectra were collected every 24 h until severe sample degradation was observed (∼2 days).

NMR Spectroscopy. NMR samples were prepared with ^{15}N-isotopically labeled protein with 10% v/v of *d*-pentane or D_2O as the lock solvent (Sigma-Aldrich, St. Louis, MO). All NMR spectra were collected at 25 °C at 600 or 700 MHz on Bruker Avance III instruments. NMR spectra of both aqueous and RM encapsulated GPx4 were collected at pH 6.0, PEBP1 was collected at pH 7.5, and ubiquitin was collected at pH values of 5.5, 6.0, 7.5, and 8.0. All NMR spectra were processed using NMRPipe[49] and analyzed using NMRFAM-Sparky.[50] Chemical shifts for ubiquitin at pH 6.0 (BMRB 25972)[51] and GPx4 (BMRB 50955)[41] were assigned from those previously published. Chemical shifts for PEBP1 were placed from those previously published at pH 4.0 (BMRB 17382), with a pH titration performed to place assignments at pH 7.5.[52] A three-dimensional HNCA was collected with $^{13}C-^{15}N$-labeled PEBP1 to confirm and complete assignments.[53] Chemical shift perturbations from ^{15}N-HSQC spectra were calculated using the following formula

$$\text{CSP} = \sqrt{(\Delta^1\text{H})^2 + \left(\frac{\Delta^{15}\text{N}}{9.8655}\right)^2}$$

where Δ^1H and $\Delta^{15}N$ are the changes in ^1H and ^{15}N chemical shifts.

Small-Angle X-ray Scattering. Samples were assembled with 75 mM total surfactant, at a molar percentage ratio of 50:50 DLPC:DPC (37.5 mM of each surfactant), with W_0 values of 15, 20, and 25 in hexane with 1.4 M hexanol. The buffer consisted of 20 mM bis−Tris pH 6.0 and 10 mM DTT, with 500 mM NaBr included in the buffer for enhanced contrast.[54] RM samples were loaded into quartz capillaries with 1.0 mm outer diameter and 0.01 mm wall thickness (Hampton Research, Aliso Viejo, CA). Experiments were performed with an Empyrean Multipurpose X-ray diffractometer with a copper anode generator (Kα = 1.54 Å), using a 0.02° divergence slit and acquired at a resolution of 0.01° per step. A three-axis $\chi-\pi-z$ stage was used for sample placement, equipped with a custom stage to accommodate capillaries. A sample containing only hexane was used for solvent subtraction. Scattering data were circularly averaged to

https://doi.org/10.1021/acs.langmuir.1c03085
Langmuir 2022, 38, 3676−3686

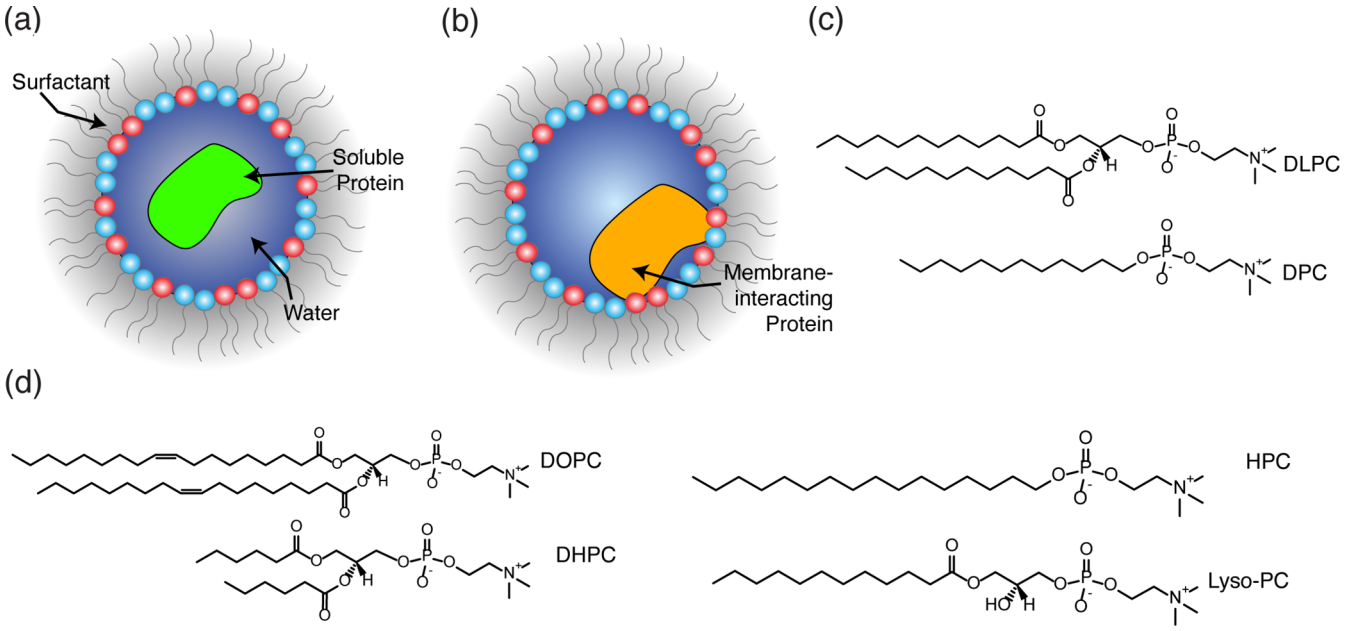

Figure 1. Two types of RM protein encapsulation and surfactants used in this study. (a) Diagram of encapsulation of an aqueous, water-soluble protein within an RM. Surfactant headgroups are depicted in blue and red. (b) Diagram of a membrane-interacting protein encapsulated within a RM and embedded into the surfactant surface. Peripheral membrane proteins are expected to interact with phosphocholine headgroups of a surfactant shell, while fully aqueous proteins are not expected to interact with the shell. (c) Structures of DLPC and DPC, the optimal surfactant mixture found in this study. (d) Structures of other surfactants trialed during this study that were found to form RMs but were less optimal for protein encapsulation or/and PMP embedment.

generate the one-dimensional scattering profile, which was evaluated using the Guinier analysis.[55]

RESULTS AND DISCUSSION

Screening for Membrane-like RM Formulations. The overall goal of this investigation was to find not only a new, highly versatile RM surfactant system that would preserve the native structure of proteins when encapsulated (Figure 1a) but one that is also able to act as a surface model for membrane-interacting proteins (Figure 1b). We began our screening for optimized membrane-mimicking RM formulations with various surfactants containing phosphocholine headgroups (Figure 1c,d), which is the most abundant headgroup of many eukaryotic membrane surfaces.[34] We initially tested DLPC and DOPC, which are similar to cellular phosphocholine lipids but contain shorter aliphatic tails, which is known to improve protein NMR performance.[29] We chose to focus on RMs formed using short-chain linear alkanes (pentane or hexane) as the solvent, which have a very low viscosity and allow optimal tumbling for protein NMR.[12] RMs are formed with relatively small amounts of water, described by W_0.[56] Our initial visual screening indicates that both DLPC and DOPC create transparent solutions in hexane, with W_0 = 20 and >800 mM hexanol as a co-surfactant, indicating that RMs are likely forming. This system is reminiscent of CTAB, which utilizes hundreds of millimolar of hexanol as a co-surfactant and contrasts AOT, which does not use hexanol, and 10MAG:LDAO, which requires only a small concentration of hexanol.[11] Next, binary systems that incorporate both two-tailed and single-tailed surfactants, such as DLPC and HPC, were screened. DLPC:HPC at several different mixture percentages, specifically 70:30, 60:40, 50:50, 40:60, and 30:70, was able to form transparent RM solutions. However, the hexanol concentrations needed were substantial even for modest W_0 values between 15 and 20, with solutions displaying clarity only at or above 1.8 M hexanol. We exchanged HPC for the shorter chain variant, DPC, and once again observed the formation of transparent RM solutions but with significantly lower hexanol concentrations (Figure S1b). The DLPC:DPC binary mixture was also tested at molar percentage ratios of 70:30, 60:40, 50:50, 40:60, and 30:70, which were all able to form clear, RM solutions. We attempted several other binary systems, specifically DHPC:HPC, DHPC:DPC, and DLPC:Lyso-PC, as well as HPC on its own, in an effort to expand the formulations that would be successful for protein encapsulation (Table S1). All conditions resulting in transparent solutions were characterized using DLS and included the following surfactant systems: DOPC, DLPC, DLPC:HPC, DLPC:DPC, DHPC:HPC, DHPC:DPC, HPC, and DLPC-Lyso-PC (Table S1). DLS results indicate that all tested formulations form monodisperse RMs with average solvodynamic diameters between ~5.4 and 8.8 nm (Figure S2).

Soluble Protein Encapsulation. To assess the compatibility of our new formulations with proteins, we first tested ubiquitin encapsulation. Successful encapsulation of proteins within the RM water core is reflected in transparent solutions and high-quality protein NMR spectra (^{15}N-HSQCs), defined by well-resolved resonances and high signal-to-noise ratios. ^{15}N-HSQC spectra are highly sensitive to protein conformations and interactions. In this study, relatively small changes in resonance chemical shifts that are structurally localized indicate an interaction with the RM.[11] A close correlation of resonances corresponding to non-interacting residues when comparing an encapsulated protein and the same protein in aqueous conditions indicates that the overall protein structure is native-like and the function is not altered within the RM. All RM-forming systems were tested for their ability to encapsulate ubiquitin. The DLPC:DPC formulation displayed high-quality

https://doi.org/10.1021/acs.langmuir.1c03085
Langmuir 2022, 38, 3676−3686

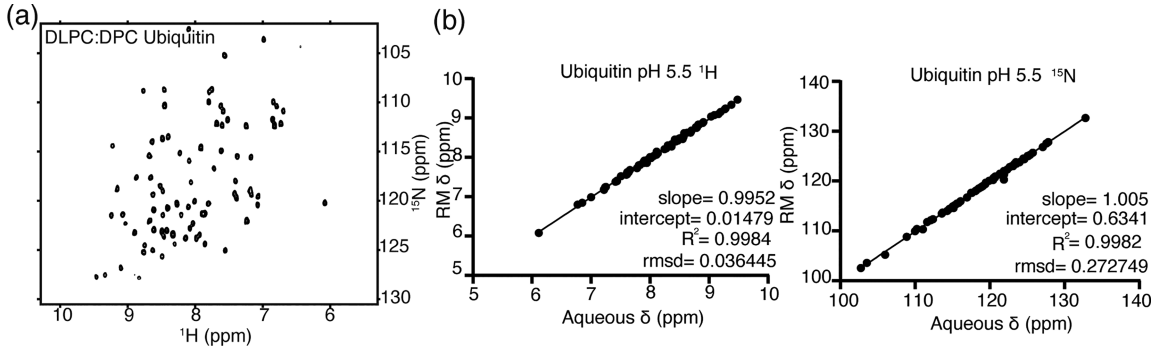

Figure 2. Aqueous protein encapsulation using DLPC:DPC. (a) ^{15}N-HSQC of ubiquitin at pH 5.5 encapsulated in 75 mM DLPC:DPC RMs at a W_0 of 15 and 975 mM hexanol. (b) Comparison of chemical shifts between ubiquitin in aqueous sample conditions and encapsulated in DLPC:DPC RMs. Comparison of both ^{1}H and ^{15}N for the aqueous and encapsulated ubiquitin indicates that the structure of ubiquitin is preserved with minimal perturbation upon encapsulation.

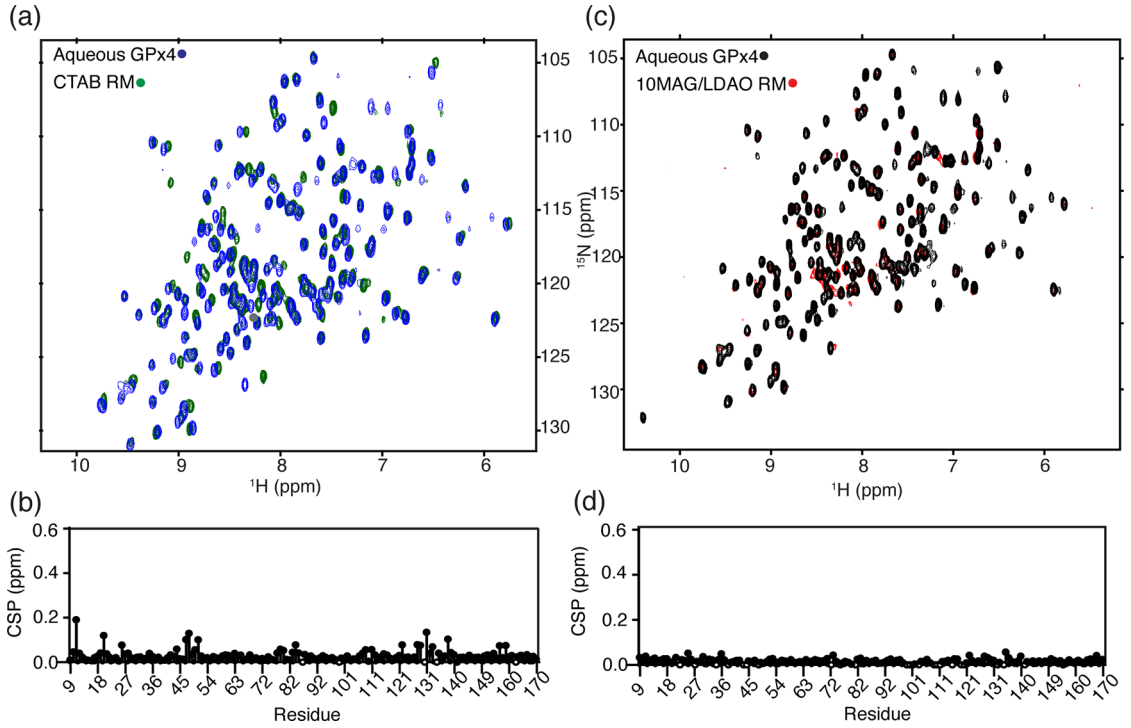

Figure 3. GPx4 has no significant interaction with current common protein-compatible RMs. (a) GPx4 was encapsulated in CTAB (150 mM surfactant, W_0 of 20, and 600 mM hexanol) and (b) displayed slight shifting that likely indicates an interaction with the bromine counter-ions. (c) GPx4 was successfully encapsulated in 10MAG:LDAO RMs (150 mM 60:40 molar percentage ratio, W_0 of 20, and 25 mM hexanol) and (d) showed nearly no relevant shifting, highlighting the utility of this system for high-fidelity encapsulation of GPx4 in the water-soluble state.

^{15}N-HSQCs with very well resolved resonances and the highest signal-to-noise ratio at molar percentage ratios of 40:60, 50:50, and 60:40, with 50:50 being optimal (Figure 2a). DLPC and DLPC:HPC also encapsulated ubiquitin successfully (Figure S3), while ubiquitin encapsulation trials using DOPC resulted in very low-intensity ubiquitin signals. DHPC:HPC, DHPC:DPC, HPC, and DLPC:Lyso-PC resulted in no substantial protein signal in ^{15}N-HSQC. Details of attempts to optimize these RM systems are included in the Supporting Information. Ultimately, the binary mixtures of single-tailed and two-tailed surfactants of DLPC:HPC and DLPC:DPC resulted in the highest quality spectra of ubiquitin.

One unique application of RMs combined with protein NMR is the ability to capture the dynamics of water on protein surfaces. A key property that enables hydration dynamics measurements is that the exchange of backbone amide hydrogens is slowed upon RM encapsulation.[27] This property reflects a slowed hydroxide-catalyzed hydrogen exchange, limiting exchange artifacts and enabling the measurement of protein surface hydration dynamics. To understand whether the DLPC:DPC system displays similar properties, we performed ubiquitin encapsulations at pH 5.5, 6.0, 7.5, and 8.0. We observed the resonance corresponding to glycine 75 broaden with the increase in pH up to disappearance at pH 7.5 in standard aqueous conditions. When encapsulated in DLPC:DPC at pH 7.5 the hydrogen exchange is slowed and the resonance is clearly visible (Figure S4c). However, at pH 8.0 the resonance corresponding to glycine 75 in both the aqueous and the encapsulated HSQCs was severely exchange broadened and not observed (Figure S4d). Glycine 75 was still visible at pH 9.0 when ubiquitin was encapsulated in AOT.[27] Therefore, while it is to a smaller degree as with AOT

https://doi.org/10.1021/acs.langmuir.1c03085
Langmuir 2022, 38, 3676−3686

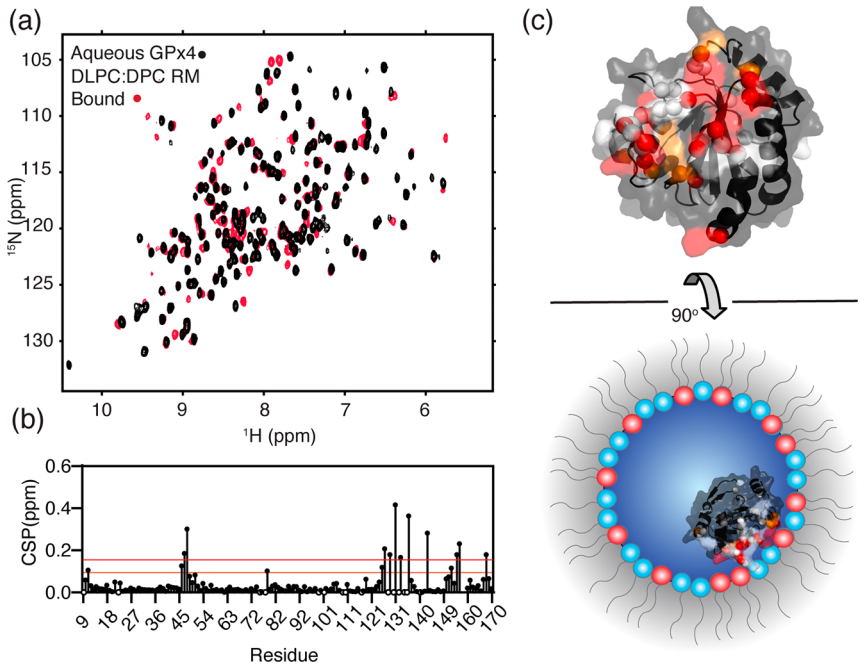

Figure 4. Membrane embedment of PMP GPx4 visualized using DLPC:DPC RMs. (a) ^{15}N-HSQC overlay of aqueous GPx4 with DLPC:DPC encapsulated GPx4 at pH 6.0. Here, 75 mM DLPC:DPC was used at a 50:50 molar percentage ratio. The W_0 for encapsulation was 20, and the hexanol concentration was 900 mM. (b) Large degrees of chemical shift perturbations are observed upon encapsulation in the membrane interaction regions, evidence that GPx4 is embedding into the surfactant shell. CSP outliers were determined by calculating a 20% trimmed mean of total CSPs plus 1σ (0.085 ppm, orange line) and 2σ (0.15, red line). (c) Structural depiction of the membrane interface and a scheme of GPx4 embedding into the surfactant shell of DLPC:DPC, which is consistent with experimental data (PDB 2OBI). Residues are colored according to the 1σ (orange) and 2σ (red) outlier cutoffs. Residues with corresponding resonances that disappear due to line broadening are depicted in white, while unperturbed residues are shown in gray.

encapsulation of ubiquitin, we do observe significant slowing of hydroxide catalyzed hydrogen exchange, suggesting that this system is compatible with measurements of protein hydration dynamics. Additionally, the range of pH values that accommodates ubiquitin encapsulation demonstrates the robustness of the DLPC:DPC RM formulation for a range of solution conditions.

Structural fidelity of RM encapsulated proteins is essential, and the sensitivity of NMR allows us to observe if any major structural perturbations occur. A strong correlation between HSQC spectra of a protein in different conditions indicates that the protein retains its native fold and function. We compared the ^{15}N and ^{1}H backbone chemical shifts of the aqueous ubiquitin HSQC and DLPC:DPC encapsulated HSQC, which revealed a well-correlated overlay of an aqueous HSQC of ubiquitin and DLPC:DPC encapsulated protein, with an R^2 value of 0.9984 for ^{1}H and 0.9982 for ^{15}N backbone resonance chemical shifts at pH 5.5, well within the benchmarks for high-fidelity protein encapsulation (Figure 2b).[11] While the majority of resonances did not shift upon encapsulation, a small subset did display chemical shift perturbations. To reveal CSP outliers, we calculated a 20% trimmed mean, with resonances greater than the trimmed mean plus 1σ and 2σ being two categories of outliers for ubiquitin at pH 6.0 (Figure S5). The 2σ cutoff of >0.097 ppm encompassed residues T9, Q49, R74, and G75. The second cutoff of >0.062 ppm included residues T12, G47, K48, L69, R72, L73, and G76. These residues do not form a continuous surface, indicating that ubiquitin is not fully embedding in the surfactant shell. Interestingly, these residues correspond well with those observed to transiently interact with amphipathic, anionic surfaces, such as those in AOT RMs and on SDS micelles.[27,57] The ubiquitin interaction observed in the DLPC:DPC RM system is further evidence in an emerging view that ubiquitin engages in weak interactions with anionic amphiphiles.

Embedment of Peripheral Membrane Proteins. To understand if protein−membrane interfacial interactions can be efficiently studied in these systems, faithful encapsulation and embedment of PMPs was tested (Figure 1b). We used GPx4 as our initial trial protein for PMP encapsulation because its membrane-binding interface is known from previous micelle- and isotropic bicelle-based experiments.[41] Encapsulation of GPx4 within the established CTAB:hexanol and 10MAG:LDAO RM systems resulted in high-quality spectra but did not display chemical shift perturbations consistent with a membrane interaction (Figure 3). A small degree of shift was observed with CTAB, most likely due to an anionic interaction with the bromine counter-ion of the surfactant, reflecting the known interaction between GPx4 and anionic phosphate (Figure 3b).[41] CTAB and 10MAG:LDAO systems were developed to encapsulate water-soluble proteins with their native fold intact while avoiding protein interactions with the RM surfactant shell; therefore, these systems are somewhat limited as membrane models, which was further confirmed with GPx4 encapsulation.[29,58]

We obtained high-quality spectra of GPx4 encapsulated in 50:50 DLPC:DPC, leading us to ultimately choose this formulation as our optimized RM system (Figures 4a and S6a). When GPx4 was encapsulated within the DLPC:HPC system, a large loss in spectral quality and signal intensity resulted, as compared to GPx4 in aqueous conditions, so we

https://doi.org/10.1021/acs.langmuir.1c03085
Langmuir 2022, 38, 3676−3686

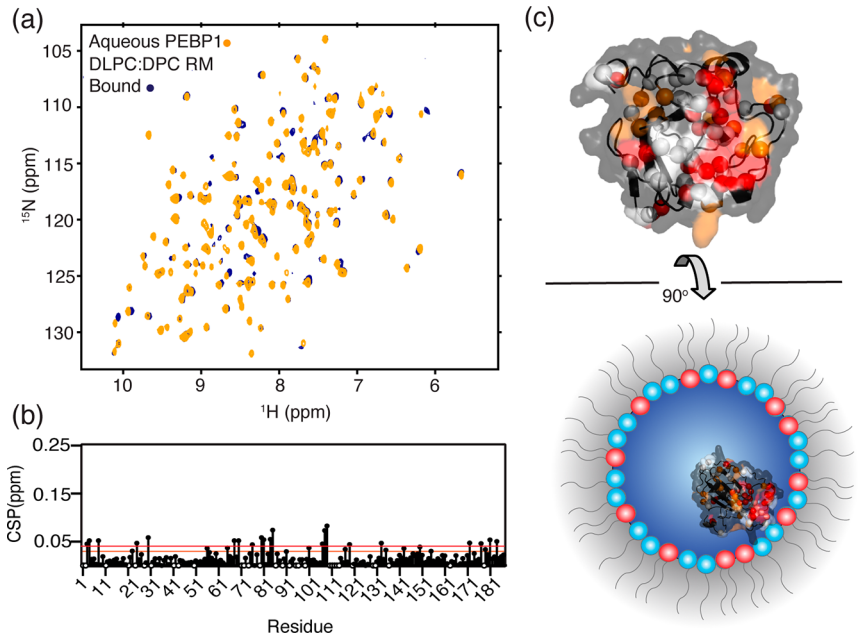

Figure 5. PMP PEBP1 surface interaction with DLPC:DPC. (a) ^{15}N-HSQC of aqueous PEBP1 overlaid with DLPC:DPC PEBP1 at pH 7.5. 75 mM DLPC:DPC was used at a 50:50 molar percentage ratio. The W_0 for encapsulation was 25, and the final hexanol concentration was 1.05 M. (b) CSPs of PEBP1 interacting with the headgroups of DLPC:DPC were calculated and mapped. CSP outliers were determined by calculating a 20% trimmed mean of total CSPs plus 1σ (0.028 ppm, orange) and 2σ (0.045 ppm, red). (c) Depiction of the membrane interface and a scheme of PEBP1 binding to the surface of the surfactant shell of DLPC:DPC, consistent with experimental data (PDB 1BD9). Residues are colored according to the 1σ (orange) and 2σ (red) outlier cutoffs. Residues with corresponding resonances that disappear due to line broadening are depicted in white, while unperturbed residues are shown in gray.

did not further pursue this mixture (Figure S7). Encapsulation of GPx4 within DLPC RMs resulted in no protein NMR signal. An overlay of aqueous GPx4 and DLPC:DPC encapsulated GPx4 showed a binding interaction that is remarkably similar to binding with DPC micelles, with key residues in both the catalytic and cationic regions showing chemical shift changes (Figures 4 and S8).[41] Minor differences in the ^{15}N-HSQC spectra of DLPC:DPC encapsulated GPx4 compared to GPx4 bound to DPC micelles are likely due to the presence of DLPC and hexanol in the RM shell (Figure S8). The CSP analysis reveals that the membrane interface is centered around G46-K48 as well as K127-W136, R152, and the structurally adjacent residue G79, as observed previously. The DLPC:DPC RM-embedded GPx4 spectrum correlates well to the spectrum of GPx4 embedded in DPC micelles, which has been shown to house enzymatically active GPx4.[41] Therefore, encapsulation within the DLPC:DPC system retains the native fold and function of membrane-embedded GPx4. These results indicate that the DLPC:DPC RM formulation embeds GPx4 nearly identically to previously investigated membrane model systems and behaves as an adequate model to house and embed membrane-interacting proteins.

Additionally, we tested PEBP1 using the optimal DLPC:DPC system (Figure 5a). Like with GPx4, we observed individual resonances shifting, indicating that there is a binding interaction between the protein and the RM. We observed shifting resonances corresponding to residues surrounding the ligand-binding pocket (Figure 5b,c), which compares well to a previously proposed membrane interface.[59] The calculated CSP outliers implicate that residues K80-H85 and V107-S109 and other structurally adjacent residues form the membrane-interacting interface of PEBP1 with the DLPC:DPC surfactant shell. Other resonances, corresponding to non-interacting residues, correlate very well, indicating that PEBP1 retains its native fold when encapsulated in the RM. While clearly indicating a membrane-binding surface, the values of the chemical shift perturbations are lower than those observed in GPx4. A difference in membrane-binding modes would account for this difference, with GPx4 loops embedding relatively deeply into the membrane and PEBP1 seemingly binding to the surface with a shallow depth of embedment. Comparison between DPC micelle bound and DLPC:DPC RM encapsulated PEBP1 reveals a high degree of correlation (Figure S9), which is a further evidence that membrane surface interactions are well-represented in this system. This second membrane-associated protein again indicates that the new DLPC:DPC RM system is a viable membrane mimic to investigate membrane interactions. Average resonance line widths and signal-to-noise ratios of GPx4 and PEBP1 in DLPC:DPC RMs compared to each protein embedded in DPC micelles are essentially unchanged. Additionally, we found that DLPC:DPC was superior for long-term stability of both GPx4 and PEBP1 compared to their stability with DPC micelles. Aqueous DPC micelle samples of GPx4 and PEBP1 were stable for less than ~2 days before the samples began to display signs of degradation. However, optimized DLPC:DPC encapsulated GPx4 and PEBP1 were stable for weeks, with our oldest samples being >1 month old and displaying no significant degradation in signal intensity. Enhanced stability suggests that the surface of the DLPC:DPC RM may be a better mimic of the biological membrane surface than the commonly used DPC micelles.[9]

RM Size and Shape Characterization. We performed SAXS experiments to understand the size, shape, and composition of the DLPC:DPC RMs. Bromine was previously shown to provide ample contrast for the characterization of the

https://doi.org/10.1021/acs.langmuir.1c03085
Langmuir 2022, 38, 3676−3686

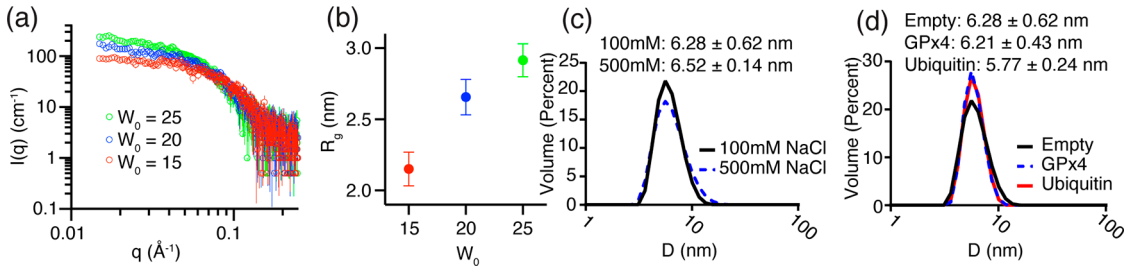

Figure 6. SAXS and DLS profiles of DLPC:DPC RMs. (a) SAXS data for 75 mM DLPC:DPC in hexane with 1.4 M hexanol and W_0 values of 15 (red), 20 (blue), and 25 (green). The major contrast component is Br^- ion from the 500 mM NaBr that was included in the aqueous phase. Error bars for the measurements are included and are not visible if they are smaller than the data symbol size. (b) Guinier analysis provides an estimate of the radius of gyration (R_g) of the bromine pseudo-shell that is known to form within the aqueous core of RMs. Increasing R_g values are observed upon increase in the water content. The R_g values estimated here are: 2.15 ± 0.12 nm for W_0 = 15, 2.66 ± 0.12 nm for W_0 = 20, and 2.92 ± 0.12 nm for W_0 = 25. (c) DLS data depicting the volume-weighted solvodynamic diameter distribution for 75 mM DLPC:DPC RMs in hexane with 1.2 M hexanol at W_0 = 20 with both 100 mM NaCl and 500 mM NaCl confirm that salt concentration does not significantly alter the size of the RMs. One representative trace is displayed, with average and error calculated from experiments collected in triplicate. (d) DLS data for DLPC:DPC in hexane with 1.2 M hexanol at a W_0 of 20 for empty RMs versus RMs containing encapsulated ubiquitin or GPx4. One representative trace is displayed, with average and error calculated from experiments collected in triplicate.

water core of RMs.[54,60] To increase the contrast for high-quality SAXS experiments, we added 500 mM NaBr to the RM aqueous phase. We collected SAXS profiles for DLPC:DPC RMs with 1.4 M hexanol and varying W_0: 15, 20, and 25. Scattering profiles are consistent with small, uniform, and roughly spherical RMs (Figure 6a).[60] Guinier analysis reveals no observable aggregation or interparticle interactions.[55] Additionally, we observed a trend of increasing radii of gyration (R_g) as W_0 is increased, consistent with previous results of other RM formulations.[60] While Br^- provides ample scattering, the distribution within the core of RMs is known to take on a "pseudo-shell" shape due to charge repulsion of the bromine ions. While this limits the usefulness of simple shape-fitting procedures, the scattering profiles here match well with those previously collected for uniform, roughly spherical CTAB RMs.[54,60] Guinier analysis of the SAXS profiles provides an estimate of the R_g of the water core, which is shown here to be 2.15 ± 0.12 nm for W_0 = 15, 2.66 ± 0.12 nm for W_0 = 20, and 2.92 ± 0.12 nm for W_0 = 25 (Figure 6b). These results are consistent with previous characterizations of the commonly used CTAB RM system, though the R_g values for the Br^- pseudo-shell of the DLPC:DPC system here are about 25% smaller than those for CTAB RMs.[60] Salt concentration is known to alter the size and stability in some RM systems.[61] Comparative DLS measurements revealed that the high salt concentrations used to enhance the contrast in SAXS experiments lead to a slightly broader size distribution but do not significantly affect the RM size (Figure 6c). Additionally, protein encapsulation results in a slight narrowing of size distribution but does not significantly change the RM size with GPx4 encapsulation and reveals a very slight size reduction (~8%) with ubiquitin encapsulation (Figure 6d). The results of SAXS experiments and Guinier analysis confirm that the DLPC:DPC RM system is not significantly aggregated, is small, and is approximately spherical and that increasing the water content increases the size of the RMs. These properties are important for protein encapsulation and other experiments where knowledge and control of the size and shape parameters are necessary.

CONCLUSIONS

Presented here are novel RM formulations that are optimized to behave as membrane mimics for interfacial studies. Among the formulations reported here, the DLPC:DPC mixture has the broadest utility as a membrane model. This system has proven to encapsulate the water-soluble protein ubiquitin with a high degree of structural fidelity, similar to other currently employed RM formulas. Membrane-interacting proteins, GPx4 and PEBP1, interact with the RM shell in a manner that reflects their expected interaction with biological membranes. Importantly, the proteins housed within the core of DLPC:DPC RMs here are stable long-term, with nearly no observable signal degradation over the course of >1 month. Embedding membrane-interacting proteins in the RMs formulated here will allow for a wide range of high-resolution studies of the interface between proteins and membranes. Additionally, these formulations may be used in many other types of interfacial investigations where it is beneficial to simulate membrane surface chemistry. The inner surface of the DLPC:DPC RM shell is composed of phosphocholine and hexanol alcohol headgroups. This chemistry well simulates the lipid environment of human cellular membranes, many of which are primarily composed of lipids with phosphocholine headgroups and cholesterol with hydroxyl headgroups. Because the protein specificity for membranes is driven by a combination of specific components and general physical properties like curvature and charge to accommodate their biologic activity, the chemical composition of a membrane model surface is key for accurate protein interaction studies.[5] The nature of membrane curvature is an important driver of certain interfacial biological processes, and the observed curvature can be quite extreme.[62,63] Concave membrane surfaces in organelle structures such as endoplasmic reticulum cisternae and Golgi tubules have minimal radii of curvature (R_c) of ~15 nm, and the protein-induced membrane curvature has been reported with an R_c as low as 10 nm or perhaps smaller.[64,65] While the RMs reported here have a significantly higher degree of curvature than found in biological membranes, with R_c ~2−3 nm, they may be useful for certain studies of small, concave environments. Optimization of protein-compatible RMs to better simulate biological membranes will allow for more accurate studies of membrane processes that are key to cellular functions. The RM formulations developed here promise to be a valuable addition to the toolbelt for membrane interfacial investigations.

https://doi.org/10.1021/acs.langmuir.1c03085
Langmuir 2022, 38, 3676−3686

■ ASSOCIATED CONTENT

Supporting Information

The Supporting Information is available free of charge at https://pubs.acs.org/doi/10.1021/acs.langmuir.1c03085.

Trialed RM formulations, detailed protein preparation protocols, and details of RM screening for some suboptimal formulations, RM phase diagrams, DLS data, and extended NMR data figures (PDF)

■ AUTHOR INFORMATION

Corresponding Author

Brian Fuglestad − *Department of Chemistry, Virginia Commonwealth University, Richmond, Virginia 23284, United States; Institute for Structural Biology, Drug Discovery and Development, Virginia Commonwealth University, Richmond, Virginia 23219, United States;* orcid.org/0000-0001-8304-8269; Email: fuglestadb@vcu.edu

Authors

Courtney L. Labrecque − *Department of Chemistry, Virginia Commonwealth University, Richmond, Virginia 23284, United States*

Aubree L. Nolan − *Department of Chemistry, Virginia Commonwealth University, Richmond, Virginia 23284, United States*

Angela M. Develin − *Department of Chemistry, Virginia Commonwealth University, Richmond, Virginia 23284, United States*

Abdul J. Castillo − *Department of Chemistry, Virginia Commonwealth University, Richmond, Virginia 23284, United States*

Adam R. Offenbacher − *Department of Chemistry, East Carolina University, Greenville, North Carolina 27858, United States;* orcid.org/0000-0001-6990-7178

Complete contact information is available at: https://pubs.acs.org/10.1021/acs.langmuir.1c03085

Notes

The authors declare no competing financial interest.

■ ACKNOWLEDGMENTS

We would like to acknowledge Carl Mayer from the Nanomaterials Characterization Core at VCU for assistance with SAXS data collection, Dr. Yun Qu for NMR assistance, and Dr. Tonie Wright for DLS assistance. We thank Dr. Ashton Cropp for generously providing the ubiquitin expression plasmid and guidance in the protein preparation. We would also like to acknowledge Grega Popovic (ECU) for his technical assistance in preparation of PEBP1. We would like to acknowledge the National Science Foundation CHE-1851916 award for support for Aubree Nolan. This research was supported by startup funds from Virginia Commonwealth University.

■ REFERENCES

(1) Corradi, V.; Sejdiu, B. I.; Mesa-Galloso, H.; Abdizadeh, H.; Noskov, S. Y.; Marrink, S. J.; Tieleman, D. P. Emerging Diversity in Lipid−Protein Interactions. *Chem. Rev.* **2019**, *119*, 5775−5848.

(2) Cheng, Y. Membrane Protein Structural Biology in the Era of Single Particle Cryo-EM. *Curr. Opin. Struct. Biol.* **2018**, *52*, 58−63.

(3) Renaud, J.-P.; Chari, A.; Ciferri, C.; Liu, W.-t.; Rémigy, H.-W.; Stark, H.; Wiesmann, C.; Remigy, H.-W.; Stark, H.; Wiesmann, C. Cryo-EM in Drug Discovery: Achievements, Limitations and Prospects. *Nat. Rev. Drug Discovery* **2018**, *17*, 471−492.

(4) Boes, D. M.; Godoy-Hernandez, A.; McMillan, D. G. G. Peripheral Membrane Proteins: Promising Therapeutic Targets across Domains of Life. *Membranes* **2021**, *11*, 346.

(5) Moravcevic, K.; Oxley, C. L.; Lemmon, M. A. Conditional Peripheral Membrane Proteins: Facing up to Limited Specificity. *Structure* **2012**, *20*, 15−27.

(6) Carpenter, E. P.; Beis, K.; Cameron, A. D.; Iwata, S. Overcoming the Challenges of Membrane Protein Crystallography. *Curr. Opin. Struct. Biol.* **2008**, *18*, 581−586.

(7) Warschawski, D. E.; Arnold, A. A.; Beaugrand, M.; Gravel, A.; Chartrand, É.; Marcotte, I. Choosing Membrane Mimetics for NMR Structural Studies of Transmembrane Proteins. *Biochim. Biophys. Acta Biomembr.* **2011**, *1808*, 1957−1974.

(8) Dufourc, E. J. Bicelles and Nanodiscs for Biophysical Chemistry. *Biochim. Biophys. Acta Biomembr.* **2021**, *1863*, 183478.

(9) Chipot, C.; Dehez, F.; Schnell, J. R.; Zitzmann, N.; Pebay-Peyroula, E.; Catoire, L. J.; Miroux, B.; Kunji, E. R. S.; Veglia, G.; Cross, T. A.; Schanda, P. Perturbations of Native Membrane Protein Structure in Alkyl Phosphocholine Detergents: A Critical Assessment of NMR and Biophysical Studies. *Chem. Rev.* **2018**, *118*, 3559−3607.

(10) Klöpfer, K.; Hagn, F. Beyond Detergent Micelles: The Advantages and Applications of Non-Micellar and Lipid-Based Membrane Mimetics for Solution-State NMR. *Prog. Nucl. Magn. Reson. Spectrosc.* **2019**, *114*, 271−283.

(11) Fuglestad, B.; Marques, B. S.; Jorge, C.; Kerstetter, N. E.; Valentine, K. G.; Wand, A. J. Reverse Micelle Encapsulation of Proteins for NMR Spectroscopy. *Methods Enzymol.* **2019**, *615*, 43−75.

(12) Wand, A. J.; Ehrhardt, M. R.; Flynn, P. F. High-Resolution NMR of Encapsulated Proteins Dissolved in Low-Viscosity Fluids. *Proc. Natl. Acad. Sci. U.S.A.* **1998**, *95*, 15299−15302.

(13) Riter, R. E.; Undiks, E. P.; Levinger, N. E. Impact of Counterion on Water Motion in Aerosol OT Reverse Micelles. *J. Am. Chem. Soc.* **1998**, *120*, 6062−6067.

(14) Nucci, N. V.; Vanderkooi, J. M. Temperature Dependence of Hydrogen Bonding and Freezing Behavior of Water in Reverse Micelles. *J. Phys. Chem. B* **2005**, *109*, 18301−18309.

(15) De, T. K.; Maitra, A. Solution Behaviour of Aerosol OT in Non-Polar Solvents. *Adv. Colloid Interface Sci.* **1995**, *59*, 95−193.

(16) Mukherjee, S.; Chowdhury, P.; DeGrado, W. F.; Gai, F. Site-Specific Hydration Status of an Amphipathic Peptide in AOT Reverse Micelles. *Langmuir* **2007**, *23*, 11174−11179.

(17) Fayer, M. D.; Levinger, N. E. Analysis of Water in Confined Geometries and at Interfaces. *Annu. Rev. Anal. Chem.* **2010**, *3*, 89−107.

(18) Orlich, B.; Schomäcker, R. Enzyme Catalysis in Reverse Micelles. *History and Trends in Bioprocessing and Biotransformation*; Springer, 2002; pp 185−208.

(19) Melo, E. P.; Aires-Barros, M. R.; Cabral, J. M. S. Reverse Micelles and Protein Biotechnology. *Biotechnol. Annu. Rev.* **2001**, *7*, 87−129.

(20) Yeung, P. S.-W.; Eskici, G.; Axelsen, P. H. Infrared Spectroscopy of Proteins in Reverse Micelles. *Biochim. Biophys. Acta Biomembr.* **2013**, *1828*, 2314−2318.

(21) Murakami, H.; Nishi, T.; Toyota, Y. Determination of Structural Parameters of Protein-Containing Reverse Micellar Solution by near-Infrared Absorption Spectroscopy. *J. Phys. Chem. B* **2011**, *115*, 5877−5885.

(22) Xu, G.; Cheng, K.; Wu, Q.; Liu, M.; Li, C. Confinement Alters the Structure and Function of Calmodulin. *Angew. Chem.* **2017**, *129*, 545−549.

(23) Peterson, R. W.; Anbalagan, K.; Tommos, C.; Wand, A. J. Forced Folding and Structural Analysis of Metastable Proteins. *J. Am. Chem. Soc.* **2004**, *126*, 9498−9499.

(24) Kelly, A. E.; Ou, H. D.; Withers, R.; Dötsch, V. Low-Conductivity Buffers for High-Sensitivity NMR Measurements. *J. Am. Chem. Soc.* **2002**, *124*, 12013−12019.
(25) Flynn, P. F.; Mattiello, D. L.; Hill, H. D. W.; Wand, A. J. Optimal Use of Cryogenic Probe Technology in NMR Studies of Proteins. *J. Am. Chem. Soc.* **2000**, *122*, 4823−4824.
(26) Fuglestad, B.; Kerstetter, N. E.; Wand, A. J. Site-Resolved and Quantitative Characterization of Very Weak Protein−Ligand Interactions. *ACS Chem. Biol.* **2019**, *14*, 1398−1402.
(27) Nucci, N. V.; Pometun, M. S.; Wand, A. J. Site-Resolved Measurement of Water-Protein Interactions by Solution NMR. *Nat. Struct. Mol. Biol.* **2011**, *18*, 245−249.
(28) Fuglestad, B.; Kerstetter, N. E.; Bédard, S.; Wand, A. J. Extending the Detection Limit in Fragment Screening of Proteins Using Reverse Micelle Encapsulation. *ACS Chem. Biol.* **2019**, *14*, 2224.
(29) Dodevski, I.; Nucci, N. V.; Valentine, K. G.; Sidhu, G. K.; O'Brien, E. S.; Pardi, A.; Wand, A. J. Optimized Reverse Micelle Surfactant System for High-Resolution NMR Spectroscopy of Encapsulated Proteins and Nucleic Acids Dissolved in Low Viscosity Fluids. *J. Am. Chem. Soc.* **2014**, *136*, 3465−3474.
(30) Kielec, J. M.; Valentine, K. G.; Babu, C. R.; Wand, A. J. Reverse Micelles in Integral Membrane Protein Structural Biology by Solution NMR Spectroscopy. *Structure* **2009**, *17*, 345−351.
(31) Valentine, K. G.; Peterson, R. W.; Saad, J. S.; Summers, M. F.; Xu, X.; Ames, J. B.; Wand, A. J. Reverse Micelle Encapsulation of Membrane-Anchored Proteins for Solution NMR Studies. *Structure* **2010**, *18*, 9−16.
(32) Van Horn, W. D.; Ogilvie, M. E.; Flynn, P. F. Use of Reverse Micelles in Membrane Protein Structural Biology. *J. Biomol. NMR* **2008**, *40*, 203−211.
(33) Harayama, T.; Riezman, H. Understanding the Diversity of Membrane Lipid Composition. *Nat. Rev. Mol. Cell Biol.* **2018**, *19*, 281−296.
(34) Casares, D.; Escribá, P. V.; Rosselló, C. A. Membrane Lipid Composition: Effect on Membrane and Organelle Structure, Function and Compartmentalization and Therapeutic Avenues. *Int. J. Mol. Sci.* **2019**, *20*, 2167.
(35) Costard, R.; Levinger, N. E.; Nibbering, E. T. J.; Elsaesser, T. Ultrafast Vibrational Dynamics of Water Confined in Phospholipid Reverse Micelles. *J. Phys. Chem. B* **2012**, *116*, 5752−5759.
(36) Costard, R.; Heisler, I. A.; Elsaesser, T. Structural Dynamics of Hydrated Phospholipid Surfaces Probed by Ultrafast 2D Spectroscopy of Phosphate Vibrations. *J. Phys. Chem. Lett.* **2014**, *5*, 506−511.
(37) Walde, P.; Giuliani, A. M.; Boicelli, C. A.; Luisi, P. L. Phospholipid-Based Reverse Micelles. *Chem. Phys. Lipids* **1990**, *53*, 265−288.
(38) Peng, Q.; Luisi, P. L. The Behavior of Proteases in Lecithin Reverse Micelles. *Eur. J. Biochem.* **1990**, *188*, 471−480.
(39) Willard, D. M.; Riter, R. E.; Levinger, N. E. Dynamics of Polar Solvation in Lecithin/Water/Cyclohexane Reverse Micelles. *J. Am. Chem. Soc.* **1998**, *120*, 4151−4160.
(40) Imai, H.; Nakagawa, Y. Biological Significance of Phospholipid Hydroperoxide Glutathione Peroxidase (PHGPx, GPx4) in Mammalian Cells. *Free Radic. Biol. Med.* **2003**, *34*, 145−169.
(41) Labrecque, C. L.; Fuglestad, B. Electrostatic Drivers of GPx4 Interactions with Membrane, Lipids, and DNA. *Biochemistry* **2021**, *60*, 2761−2772.
(42) Keller, E. T.; Fu, Z.; Brennan, M. The Role of Raf Kinase Inhibitor Protein (RKIP) in Health and Disease. *Biochem. Pharmacol.* **2004**, *68*, 1049−1053.
(43) Jones, R.; Hall, L. A 23 KDa Protein from Rat Sperm Plasma Membranes Shows Sequence Similarity and Phospholipid Binding Properties to a Bovine Brain Cytosolic Protein. *Biochim. Biophys. Acta Protein Struct. Mol. Enzymol.* **1991**, *1080*, 78−82.
(44) Vallée, B. S.; Tauc, P.; Brochon, J. C.; Maget-Dana, R.; Lelièvre, D.; Metz-Boutigue, M. H.; Bureaud, N.; Schoentgen, F. Behaviour of Bovine Phosphatidylethanolamine-Binding Protein with Model Membranes. Evidence of Affinity for Negatively Charged Membranes. *Eur. J. Biochem.* **2001**, *268*, 5831−5841.
(45) Araki, Y.; Vierulk, M. E.; Rankin, T. L.; Tulsiani, D. R. P.; Orgebin-Crist, M.-C. Isolation and Characterization of a 25-Kilodalton Protein from Mouse Testis: Sequence Homology with a Phospholipid-Binding Protein. *Biol. Reprod.* **1992**, *47*, 832−843.
(46) Frayne, J.; Ingram, C.; Love, S.; Hall, L. Localisation of Phosphatidylethanolamine-Binding Protein in the Brain and Other Tissues of the Rat. *Cell Tissue Res.* **1999**, *298*, 415−423.
(47) Franjo, C.; Jimenez, E.; Iglesias, T. P.; Legido, J. L.; Paz Andrade, M. I. Viscosities and Densities of Hexane+ Butan-1-Ol,+ Hexan-1-Ol, And+ Octan-1-Ol at 298.15 K. *J. Chem. Eng. Data* **1995**, *40*, 68−70.
(48) Singh, R. P.; Sinha, C. P. Dielectric Behavior of the Binary Mixtures of N-Hexane with Toluene, Chlorobenzene and 1-Hexanol. *J. Chem. Eng. Data* **1982**, *27*, 283−287.
(49) Delaglio, F.; Grzesiek, S.; Vuister, G. W.; Zhu, G.; Pfeifer, J.; Bax, A. NMRPipe: A Multidimensional Spectral Processing System Based on UNIX Pipes. *J. Biomol. NMR* **1995**, *6*, 277−293.
(50) Lee, W.; Tonelli, M.; Markley, J. L. NMRFAM-SPARKY: Enhanced Software for Biomolecular NMR Spectroscopy. *Bioinformatics* **2015**, *31*, 1325−1327.
(51) Surana, P.; Das, R. Observing a Late Folding Intermediate of Ubiquitin at Atomic Resolution by NMR. *Protein Sci.* **2016**, *25*, 1438−1450.
(52) Yi, C.; Peng, Y.; Guo, C.; Lin, D. 1H, 13C, 15N Backbone and Side-Chain Resonance Assignments of the Human Raf-1 Kinase Inhibitor Protein. *Biomol. NMR Assign.* **2011**, *5*, 63−66.
(53) Kay, L. E.; Ikura, M.; Tschudin, R.; Bax, A. Three-Dimensional Triple-Resonance NMR Spectroscopy of Isotopically Enriched Proteins. *J. Magn. Reson.* **2011**, *213*, 423−441.
(54) Fuglestad, B.; Gupta, K.; Wand, A. J.; Sharp, K. A. Characterization of Cetyltrimethylammonium Bromide/Hexanol Reverse Micelles by Experimentally Benchmarked Molecular Dynamics Simulations. *Langmuir* **2016**, *32*, 1674−1684.
(55) Guinier, A.; Fournet, G.; Yudowitch, K. *Small-Angle Scattering of X-Rays*; John Wiley & Sons, Inc.: New York, 1955.
(56) Feitosa, E.; Catelam, K. T.; Hasmann, F. A.; Johansson, H.-O.; Roberto, I. C.; Pessoa, A. J. Phase Diagrams of a CTAB/Organic Solvent/Buffer System Applied to Extraction of Enzymes by Reverse Micelles. *J. Chromatogr. B: Anal. Technol. Biomed. Life Sci.* **2008**, *862*, 58−63.
(57) Shaw, B. F.; Schneider, G. F.; Arthanari, H.; Narovlyansky, M.; Moustakas, D.; Durazo, A.; Wagner, G.; Whitesides, G. M. Complexes of Native Ubiquitin and Dodecyl Sulfate Illustrate the Nature of Hydrophobic and Electrostatic Interactions in the Binding of Proteins and Surfactants. *J. Am. Chem. Soc.* **2011**, *133*, 17681−17695.
(58) Lefebvre, B. G.; Liu, W.; Peterson, R. W.; Valentine, K. G.; Wand, A. J. NMR Spectroscopy of Proteins Encapsulated in a Positively Charged Surfactant. *J. Magn. Reson.* **2005**, *175*, 158−162.
(59) Banfield, M. J.; Barker, J. J.; Perry, A. C.; Brady, R. L. Function from Structure? The Crystal Structure of Human Phosphatidylethanolamine-Binding Protein Suggests a Role in Membrane Signal Transduction. *Structure* **1998**, *6*, 1245−1254.
(60) Fuglestad, B.; Gupta, K.; Wand, A. J.; Sharp, K. A. Water Loading Driven Size, Shape, and Composition of Cetyltrimethylammonium/Hexanol/Pentane Reverse Micelles. *J. Colloid Interface Sci.* **2019**, *540*, 207−217.
(61) Ridley, R. E.; Fathi-Kelly, H.; Kelly, J. P.; Vasquez, V. R.; Graeve, O. A. Predicting Destabilization in Salt-Containing Aqueous Reverse Micellar Colloidal Systems. *ACS Earth Sp. Chem.* **2021**, *5*, 2223−2232.
(62) McMahon, H. T.; Boucrot, E. Membrane Curvature at a Glance. *J. Cell Sci.* **2015**, *128*, 1065−1070.
(63) Antonny, B. Mechanisms of Membrane Curvature Sensing. *Annu. Rev. Biochem.* **2011**, *80*, 101−123.
(64) Yesylevskyy, S.; Khandelia, H. EnCurv Simple Technique of Maintaining Global Membrane Curvature in Molecular Dynamics Simulations. *J. Chem. Theory Comput.* **2021**, *17*, 1181−1193.

https://doi.org/10.1021/acs.langmuir.1c03085
Langmuir 2022, 38, 3676−3686

(65) Blood, P. D.; Voth, G. A. Direct Observation of Bin/Amphiphysin/Rvs (BAR) Domain-Induced Membrane Curvature by Means of Molecular Dynamics Simulations. *Proc. Natl. Acad. Sci. U.S.A.* **2006**, *103*, 15068−15072.

https://doi.org/10.1021/acs.langmuir.1c03085
Langmuir 2022, 38, 3676−3686